NUMERICAL STUDY OF A DIFFRACTION PROBLEM BY A MODIFIED METHOD OF NON-ORTHOGONAL SERIES*

R. S. POPOVIDI and Z. S. TSVERIKMAZASHVILI

(Received 24 July 1975)

The possibility of using a method of non-orthogonal series for the numerical solution of two-dimensional electromagnetic wave diffraction problems is considered, in the case when the characteristic dimensions of the body are comparable with wavelength of the incident waves.

One method of reducing a boundary value problem directly to the solution of a system of linear algebraic equations is the method of non-orthogonal series, the essence of which lies in representing the solution of the problem as an expansion in some system of complete, linearly independent, non-orthogonal functions, and in defining the coefficients of the expansion from the boundary conditions (see [1], pp. 23-29).

The basic idea of the present method is as follows. Let the diffraction problem amount to finding the solution, outside the body D, bounded by the surface S, of the equation

$$L[U] = 0 \tag{1}$$

with the boundary condition

$$P[U]_S = f(q)$$

and the radiation condition at infinity, where L and P are given differential operators, and U is a vector or scalar function.

Assume that a system $\{V_n(M)\}$ of particular solutions of Eq. (1) exists, such that

$$\{\varphi_n(q)\} = \{P[V_n]|_{q\in S}\}$$

forms a complete system in S, i.e., the function $f(q)$ can be approximated by the linear combination of $\varphi_n(q)$. Then the solution of Eq. (1) can be sought as a superposition of functions $V_n(M)$:

$$u_N(M) = \sum_{n=0}^{N} a_n V_n(M), \tag{2}$$

and the unknown coefficients a_n can be found from the boundary conditions.

An original method of choosing the basis functions $V_n(M)$ can be found in [2] . If we construct in the domain D a closed surface S, and choose inside S a countable and everywhere dense set of points $\{M_n\}$, on an arbitrary surface S_0, we can take as the basis functions $V_n(M)$ the fundamental solutions of the Helmholtz equation with singularities at the points M_n:

$$V_n(M) = \exp[ikR(M, M_n)]/R(M, M_n), \tag{3}$$

where $R(M, M_n)$ is the distance between the points M and M_n. It was shown in [2] that the sequence of non-orthogonal functions (3) is linearly independent and complete.

The number of concrete problems solved with the aid of the functions (3) is not yet sufficient for a valid conclusion to be drawn about the efficiency of the method for the numerical solution of a wide range of problems.

It is important to be able to find the unknown coefficients a_n such that the convergence of the series (2) is optimized. We mentioned above that the coefficients are defined from the boundary conditions, which can be specified continuously over the whole of S, though, to simplify the numerical realization of the problem, it is possible to specify them at a finite number of points, while using the method of collocation [3].

In the present paper we verify the method by solving the classical problem of diffraction at a homogeneous, ideally conducting, infinite cylinder. With the aid of numerical experiments, we study the convergence of the results of solving the problem in the range of variation of the characteristic size of the body mentioned above. In addition, we analyze the numerical experiments with a view to finding methods of selecting the surface S_0 and arranging the points M_n on the surface.

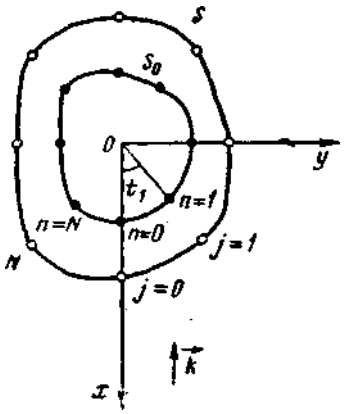

FIG. **1.**

1. The problem and its solution in general form

Let an E_z - polarized electromagnetic wave of unit amplitude

$$E_z^i = \exp[-i(kx + \omega t)]; \tag{1.1}$$

be incident from the side $x > 0$ (Fig. 1) on an ideally conducting cylinder of infinite length with a contour of normal cross-section S; henceforth, the time factor $\exp(-i\omega t)$ will be omitted.

We locate the set of points $\{M_n\}$ along the contour S_0, taken inside S, defining the position of each point in the xoy plane by means of the parameter t_n:

$$x_n = x(t_n), \quad y_n = y(t_n).$$

In accordance with [1,2], and recalling that, in the two-dimensional case, the fundamental solution of the Helmholtz equation is the Hankel cylindrical function of zero order, the expression for the field scattered by the cylinder can be written as

$$E_z^s = \sum_{n=0}^{N} a_n H_0^{(1)}[kR_n(x,y)] \tag{1.2}$$

(the kind of function $H_0^{(1)}$ is determined by the sign of the time factor of the incident wave $\exp(-i\omega t)$). Here, $a_n = a_n' + ia_n''$ are the unknown complex coefficients, while

$$R_n(x,y) = [(x - x_n)^2 + (y - y_n)^2]^{1/2},$$

where x and y are the coordinates of the observation point.

To find the coefficients a_n, we require that the tangential component of the total field on the cylinder surface vanish at a finite number of points, equal to the number of singular points:

$$(E_z^i + E_z^s)\Big|_{\substack{x=x(t_j) \\ y=y(t_j),\ j=0,1,\ldots,N}} = 0 \tag{1.3}$$

We separate the real and imaginary parts from this system of complex equations:

$$\begin{aligned} \sum_{n=0}^{N} \{a_n' J_0[kR_n(x_j,y_j)] - a_n'' N_0[kR_n(x_j,y_j)]\} &= -\cos(kx_n), \\ \sum_{n=0}^{N} \{a_n' N_0[kR_n(x_j,y_j)] + a_n'' J_0[kR_n(x_j,y_j)]\} &= -\sin(kx_n), \end{aligned} \tag{1.4}$$

where J_0 and N_0 are the Bessel and Neumann functions of zero order.

Since the number of pairs of equations in (1.4) is equal to the number of pairs of unknowns, a computer solution for the coefficients a_n' and a_n'' presents no difficulties.

After finding the expansion coefficients, it is easy to find the value of the scattered field at an arbitrary point of the near zone, this value is the total value of the fields (1.1) and (1.2):

$$E(x,y) = \exp(-ikx) + \sum_{n=0}^{N} a_n H_0^{(1)}[kR_n(x,y)] \tag{1.5}$$

The field amplitude at any point *M(x, y)* is equal to the modulus of the expression (1 .5):

$$E_0(x,y) = \{[\mathrm{Re}\,E(x,y)]^2 + [\mathrm{Im}\,E(x,y)]^2\}^{1/2}, \tag{1.6}$$

while its part is equal to the argument, up to 2π:

$$\varphi_e = arctg\frac{\mathrm{Im}\,E(x,y)}{\mathrm{Re}\,E(x,y)} + 2\pi q, \quad q = 0,1,\ldots .$$

We find the polar diagram (the field in the far zone) from (1.2) by using the asymptotic form of the Hankel function for large values of the argument:

$$H_0^{(1)}(z) \approx (2/\pi z)^{1/2} \exp[i(z - \pi/4)].$$

After simple transformations, we find that the modulus squared of the field, scattered at an angle ψ to the x axis, is

$$|F(\psi)|^2 = \left[\sum_{n=0}^{N}(a'_n \cos\chi + a''_n \sin\chi)\right]^2 + \\ + \left[\sum_{n=0}^{N}(-a'_n \sin\chi + a''_n \cos\chi\right]^2, \tag{1.7}$$

where $\chi = k(x_n \cos\psi + y_n \sin\psi)$.

The polar diagram will be normalized throughout with respect to $\psi = 0$.

2. Diffraction at a circular cylinder

In the case of a circular cylinder, the contour S of the normal cross-section is a circle of radius a. As S_0 we shall take a circle of radius a_0, concentric with $S(a_0 < a)$. Then, the coordinates of the singular points are

$$x_n = a_0 \cos(t_n), \quad y_n = a_0 \sin(t_n), \tag{2.1}$$

and the coordinates of the collocation points are

$$x_j = a\cos(t_j), \quad y_j = a\sin(t_j), \tag{2.2}$$

where

$$\left.\begin{matrix} t_n \\ t_j \end{matrix}\right\} = \frac{2\pi}{N+1} \times \begin{cases} n, \\ j, \end{cases} \quad n, j = 0,1,...,N.$$

We shall first see how the field in the far zone (expression (1.7)) depends on the number of singular points, and hence, on the collocation points, i.e., we investigate the convergence of the solutions of the problems.

Studies have shown that the nature of the convergence of the solutions is independent of the scattering angle ψ, so that, unless specially stipulated, all our results will refer to the case $\psi = 90^\circ$.

The numerical results of computing the dependence of the far zone normal field on the number N of collocation points for different values of the relative perimeter of the cylinder $ka = 2\pi a/\lambda$ (λ is the incident wavelength), show that the rate of convergence of the results depends very much on the relative perimeter. For instance, for ka=0.5 stabilization of 9 places after the decimal point sets in at N=12, for ka=2.2 at N=25, and for ka=8.0, at N=54. It may be mentioned here that the stabilization of two places, sufficient for engineering calculations, sets in respectively at N=3, N=9, and N=21. Consequently, an increase in the perimeter ka demands an increase in the number of terms in the expansion (1.2) in order to obtain a stable solution. When N is increased further, up to N_{max} = 70, the results of the solution remain unchanged.

It was found by comparison with the results obtained from the expression for the exact solution [4] that, in the range of perimeters ka investigated, 6 decimal places were the same in the worst case.

Studies also showed that the rate of convergence of the results, when the relative perimeter value is

fixed, depend on the radius a_0. For convenience, we shall introduce the dimensionless characteristic parameter $b=a_0/a$ (the ratio of the radii of the circles S_0 and S).

In Fig. 2 we plot curves of the minimum number of terms in the expansion, needed for stabilization of 6 decimal places, against the parameter b. It can be seen that the curves are so to speak bounded on the left, i.e., at some "critical" value of b the value N_{min} falls sharply to the minimum, then increases smoothly as the parameter b increases. For $b < b_{cr}$, 6 places are not stabilized in the present case for any investigated value of N. For instance, for ka=0.5 (curve 1 of Fig. 2), $b_{cr} \approx 0.02$; for ka=2.2 (curve 2), $b_{cr} \approx 0.1$; and for ka=8.0 (curve 3), $b_{cr} \approx 0.32$.

For each curve at Fig. 2 a minimum range can be isolated, within which N_{min} remains constant to within 1—2 units. The interval Δb is roughly the same for all ka. As the perimeter ka increases, the edges of the interval move towards larger values of the parameter b.

Obviously, as less accuracy is demanded for the results, the interval Δb widens on either side. The curves of Fig. 3, which show the dependence of the minimum number of expansion terms on the parameter b for different accuracies of the results, confirm what has been said (here, ka = 8.0). The curve 1 corresponds to stabilization of 6 decimal places ($\Delta b \approx 0.2$), curve 2 to stabilization of 4 places ($\Delta b \approx 0.4$), and curve 3 to stabilization of 2 places ($\Delta b \approx 0.55$).

It is interesting to observe that, for stabilization of 2 places, with fixed ka, the value of the parameter b (within the range $0.2 < b < 0.8$) is virtually of no importance (see Fig. 3).

3. Field of the circular cylinder in the near zone

From expression (1.6) we plotted a picture of the lines of equal amplitudes (Fig. 4) in the immediate neighborhood of the cylinder surface. A comparison with the similar picture obtained from the expression of the exact solution [4] shows complete identity of the lines of equal amplitude.

In Fig. 4 we also show the amplitude picture of the field inside the cylinder, which is the analytic continuation of the field outside. The aim of the picture is to show that the field amplitude, which is a minimum on the surface, increases uniformly as we move away in either direction along the normal to the surface, while the lines of equal amplitude nowhere intersect the cylinder surface.

By virtue of condition (1.3), the value of the total field at the collocation points is zero, while it is naturally non-zero between these points. Obviously, for best approximation of the problem, the field value on the cylinder surface between the collocation points should tend to zero.

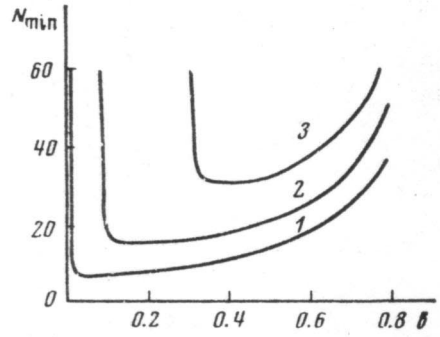

FIG. 2.

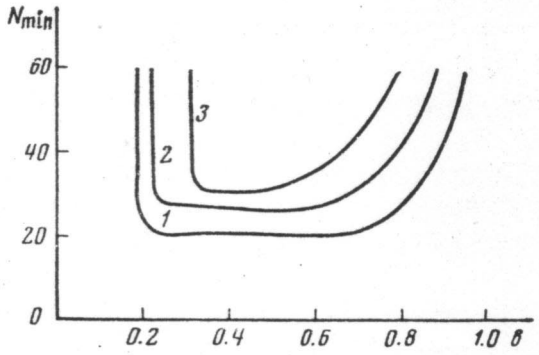

FIG. 3

In Fig. 5 we show the dependence of the field amplitude on the surface on the parameter t, denoting the polar angle (here, $ka = 0.5$). Since the picture is symmetric about $t = \pi$, the curves are only plotted for $0 \leq t \leq \pi$. The field amplitude, which, by condition (1.3), is zero at the collocation points, increases smoothly and reaches a maximum on the contour S between the points. As the number N of collocation points increases, the field amplitude maximum on the contour falls sharply. It may be mentioned that the nature of the curves is similar in the case of the other perimeter ka values studied.

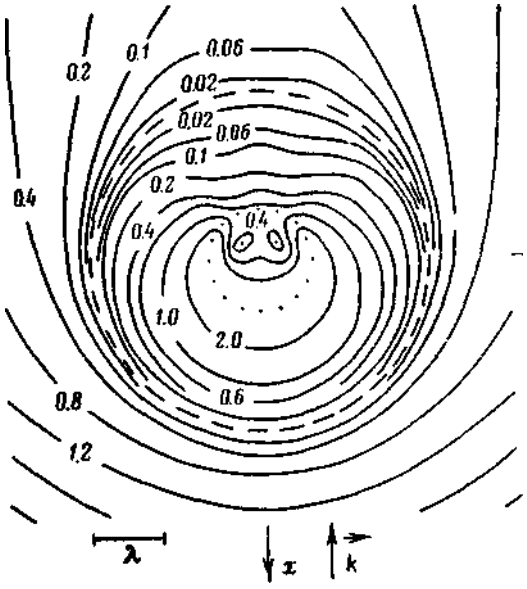

FIG. 4.

In Fig. 6, *a* we show a family of envelopes of the above curves (Fig. 5), in the case ka = 4.0. Here, the parameter value b=0.3 is taken from the optimal interval (see Table 2) for the given relative perimeter. When the number of collocation points is increased by 5 units, the value of the maximum of the envelope falls by more than one order, so that, to make the picture easier to read, the curves are plotted in different scales, depending on the factor γ in the field amplitude (see Fig. 6, *a*). Notice that the decrease in the envelope maximum occurs until N=30, then "saturation" sets in. Moreover, whereas the envelope maximum occurs at t = 90° for a small number N of points, when N is large the number of the maxima increases and they move towards t = 0° and t = 180°, while an envelope minimum occurs at t = 90°. It may be noted here that any degree of uniformity of the amplitude distribution can be achieved by varying the disposition of the collocation points on the contour.

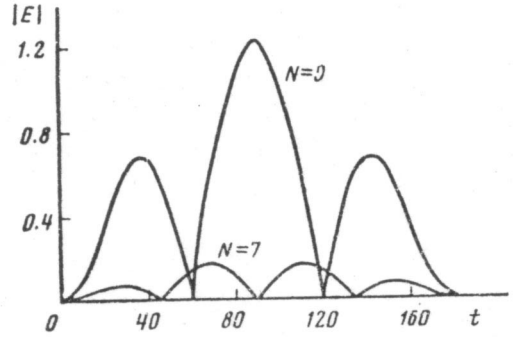

FIG. 5.

TABLE 1

N	***b***		
	0.1	0.3	0.8
5	1.336 978 578	1.337 427 156	1.277 701 752
10	0.017 120 320	0.165 098 094	0.316 351 032
15	0.003 979 581	0.006 916 239	0.067 909 472
20	0.003 062 651	0.000 199 397	0.016 129 752
25	0.001 950 072	0.000 002 550	0.004 059 222
29	0.001 105 841	0.000 000 745	0.001 401 343
30	0.076 922 213	0.082 849 989	0.080 845 521
31	0.000 545 988	0.000 000 576	0.000 816 937
35	0.000 408 479	0.000 000 307	0.000 293 116
40	0.000 935 029	0.000 000 441	0.000 622 325

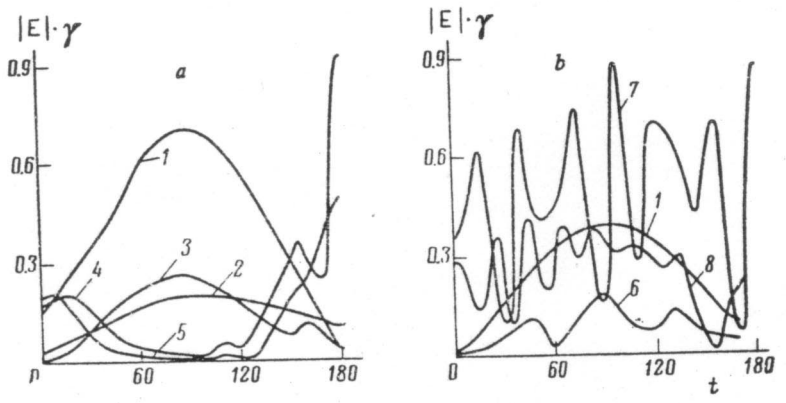

FIG. 6.

Envelopes: *1*- for N=15, $\gamma = 10^{-2}$; *2* - for N=20, $\gamma = 10^{-3}$;

3- for N=25, $\gamma = 10^{-5}$; *4* - for N=30, $\gamma = 10^{-6}$; *5*- for N=35, $\gamma = 10^{-6}$;

6- for N=25, $\gamma = 10^{-3}$; *7*- for N=30, $\gamma = 10^{-3}$; *8* - for N=35, $\gamma = 10^{-3}$.

In Fig. 6, b we plot the same family of curves but with the parameter value b = 0.1, i.e., when the convergence of the results is worst. Here, for small N, the curves are smooth, whereas with N, the curves are smooth, whereas with N=15 the boundary conditions are "better" satisfied than for b = 0.3, since the envelope maximum is in this case smaller. As the number N of collocation points increases, the envelope curves start to oscillate. Comparison of the cases considered shows that, given the same values of N, the amplitude is 2-3 orders higher in the second case. A similar effect occurs for larger values of the relative perimeter.

In Table 1 we show the dependence of the maximum deviation of the field amplitude at the cylinder surface relative to the amplitude values at the collocation points

$$H = \max_{0 \le i \le \pi} \left| E_0(t) - E_0(t_j) \right|$$

on the number of terms in expression (1.2). For some values of N, overshoots in the results are observed (in Table 1, at N = 30).

It is clear from the table that the minimum values of the deviation H are obtained for the parameter value b = 0.3 taken from the optimal interval (see Fig. 2); for the values b = 0.1 and, 0.8, the field amplitude maximum H is much greater.

The above results reveal that we are justified in using the collocation method for satisfying the boundary conditions, since the maxima of the field amplitude over the contour (in the case when the result is stabilized) is less than the amplitude at a distance 0.1 λ (λ is the incident wavelength) from the cylinder surface in the worst case, the reduction being by a factor 10^{-4}.

4. Diffraction at an elliptic cylinder

The convergence of the results of Section 2 can be explained to some extent by the circular symmetry of the body, so that it is of interest to examine the convergence in the case of a body with

a non-circular contour. As the contour S we shall take the ellipse with semi-axes a and c; as S_0 we take the ellipse with semi-axes a_0 and c_0, similar to the contour of the normal cross-section of the body; $c_0/a_0=c/a=\eta$ is the ellipticity.

Expressions (2.1) and (2.2) take the respective forms

$$x_n = a_0 \cos(t_n), \qquad y_n = \frac{1}{\eta} a_0 \sin(t_n),$$

$$x_j = a \cos(t_j), \qquad y_j = \frac{1}{\eta} a \sin(t_j).$$

As might be expected, numerical experiments showed that the convergence of the results for the elliptic cylinder is worse than for the circular cylinder. The number of stabilized places falls whether η increases or decreases (η = 1 is the circular case). For instance, with η = 1.1 and η = 0.9 (throughout, ka = 4.0), 8 places are stabilized, with η = 1 .4, 5 places are stabilized, and with η = 0.6, 4 places are stabilized. To obtain a clear-cut comparison between the results for the circular and elliptic cylinders, we introduce the quantity.

Where $F(\psi_i)$ is the field value with given accuracy $F^N(\psi_i)$ is the field value with fixed N, and $b = a_0 / a = c_0 / c$ has the same meaning as in the previous sections. Obviously, the best results will be obtained as $R^N \to 0.$

In Figs. 7 and 8 we show the dependence of R^N on the parameter b for different values of the ellipticity η (the accuracy of the results $e = 10^{-4}$).

$$R^N(b,\eta) = \max\left|F(\psi_i) - F^N(\psi_i)\right|,$$

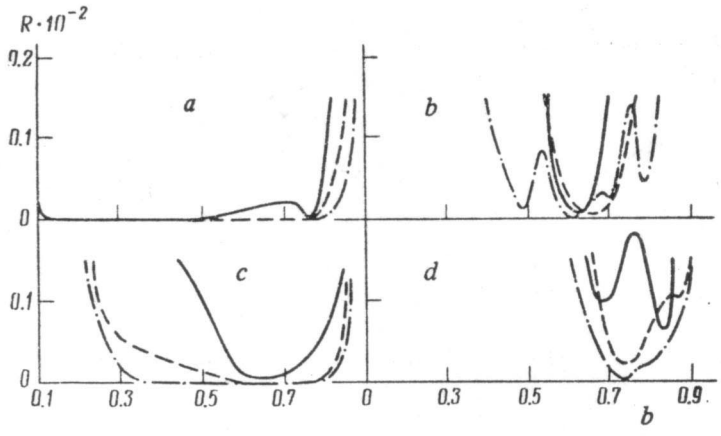

FIG. 7

Dependence of R^N on b: -N = 20

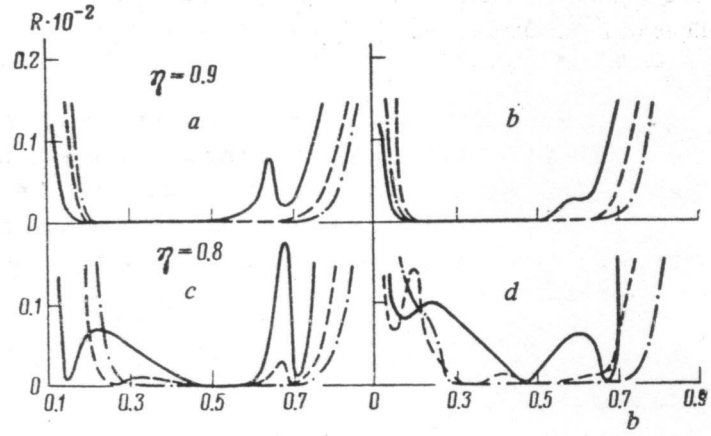

FIG. 8

$---N=25$, $-\cdot-N=30$

In the circular case, $\eta = 1$ (Fig. 7, *a*), $R^N \sim 0$ approximately over the entire range of variation of the parameter b, $0.1<b<0.8$. For $\eta \neq 1$ ($\eta = 0.7$, in Fig. 7, *b*, $\eta = 1.2$ in Fig. 7, *c*) the range of b where $R^N \sim 0$ is smaller, while in the case $\eta = 1.4$ (Fig. 7, *d*) we have $R^N \sim 0$ only at the single point $b = 0.73$ and only for $N = 30$.

Studies showed that the results also deteriorate in the case when S and S_0 are not similar figures. In Fig. 8 we give curves of R^N against the parameter b for two sorts of disposition of S and S_0 : 1) S and S_0 are similar concentric ellipses (Fig. 8, *a*, *c*), and 2) S is an ellipse, and S_0 is a circle of radius a_0 (Fig. 8, *b*, *d*; $\eta = 0.9$ in Fig. 8, *a*, b; $\eta = 0.8$ in Fig. 8, *c*, *d*). It is clear that, the more η differs from unity, the greater the difference between the pictures obtained. It must be said, furthermore, that, in the case $\eta = 0.7$, a similar dependence cannot be obtained in the second example, even with reduced accuracy.

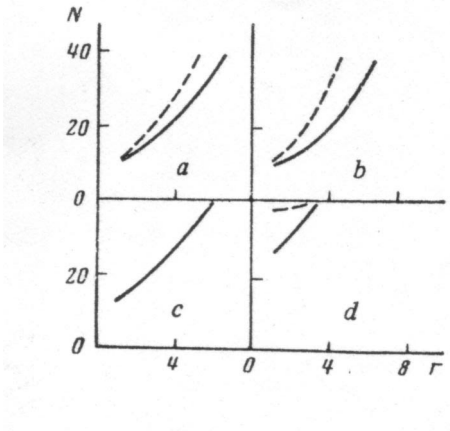

FIG. 9.

Dependence of n on N: version 1, --- version 2

The difference between the two examples is seen more clearly in Fig. 9, where we plot curves of the order n of the stabilized place of the result against the number N of collocation points, at which the

stabilization occurs. Here again we see that the difference is more marked, the larger the difference of η from unity (η = 0.9 in Fig. 9, *a*, and η = 0.8 in Fig. 9, *b*).

In the case η = 0.7 (Fig. 9, *c*) it is not possible to obtain the curve in question for the second example, except in the case b = 0.35 (Fig. 9, *d*). The explanation for all this is the fact, shown by our studies, that to obtain stable results in the elliptic case, the value of the parameter b has to be increased. But in the case of Example 2, for some value b > 0.4-0.5, the contour S_0 tends along the x axis (η > 1) or along the y axis (η < 1) to the contour S, and departs beyond its limits, which has a serious effect on the results.

Obviously, to obtain the best results by the method described, the contours S and S_0 must be similar and concentric figures.

In conclusion, the author thanks A. S. Il'inskii for useful advice and discussions.

Translated by D. E. Brown.

REFERENCES

SVESHNIKOV, A. G., and IL'INSKII, A. S., *Four lectures on numerical methods in diffraction theory* (Chetyre lektsii po chislennym metodam v teorii difraktsii), Izd-vo LGU, Leningrad, 1972.

KUPRADZE, V. D., On the approximate solution of problems of mathematical physics, *Usp. mat. nauk*. 22, No. 2 (134), 59-107, 1967.

VORONIN, V. V., and TSETSOKHO, V. A., An interpolation method of solving an integral equation of the 1st kind with a logarithmic singularity, *Dokl. Akad. Nauk SSSR,* 216, No. 6, 1209-1211, 1974.

POTEKHIN, A. I., *Some problems of electromagnetic wave diffraction* (Nekotorye zadachi difraktsii elektro*magnitnykh voln),* Sov. radio, Moscow, 1948.